ORIGINAL PAPER

Effect of plasticizer on structural and electrical properties of nanocomposite solid polymer electrolytes

Dillip K. Pradhan · B. K. Samantaray ·
R. N. P. Choudhary · N. K. Karan · Reji Thomas ·
R. S. Katiyar

Abstract The solid polymer electrolyte films based on polyethylene oxide, $NaClO_4$ with dodecyl amine modified montmorillonite as filler, and polyethylene glycol as plasticizer were prepared by a tape casting method. The effect of plasticization on structural, microstructural, and electrical properties of the materials has been investigated. A systematic change in the structural and microstructural properties of plasticized polymer nanocomposite electrolytes (PPNCEs) on addition of plasticizer was observed in our X-ray diffraction pattern and scanning electron microscopy micrographs. Complex impedance analysis technique was used to calculate the electrical properties of the nanocomposites. Addition of plasticizer has resulted in the lowering of the glass transition temperature, effective dissociation of the salt, and enhancement in the electrical conductivity. The maximum value of conductivity obtained was $\sim 4.4 \times 10^{-6}$ S cm^{-1} (on addition of $\sim 20\%$ plasticizer), which is an order of magnitude higher than that of pure polymer nanocomposite electrolyte films (2.82×10^{-7} S cm^{-1}). The enhancement in conductivity on plasticization was well correlated with the change in other physical properties.

D. K. Pradhan · N. K. Karan · R. Thomas · R. S. Katiyar (✉)
Department of Physics and Institute for Functional Nanomaterials,
University of Puerto Rico,
San Juan, PR 00931, USA
e-mail: rkatiyar@uprrp.edu

B. K. Samantaray · R. N. P. Choudhary
Department of Physics, Indian Institute of Technology,
Kharagpur 721302, India

Introduction

Ionically conducting solid polymer electrolytes (SPEs) are technologically important for a wide variety of energy storage/conversion devices, such as rechargeable batteries, fuel cells, supercapacitors, hybrid power sources, etc. [1–6]. However, the main drawback of polymer electrolytes is the low ionic conductivity at ambient temperature. Therefore, achievement of stable and higher ionic conductivity ($\sim 10^{-3}$ S cm^{-1}) in SPEs near ambient temperature is still a major challenge for their practical applications. The main reasons for the poor ionic conductivity in SPEs may be due to simultaneous mobility of cations and anions (dual ion conduction), neutral ions aggregation (i.e., ion pair formation), high degree of crystallinity, etc. Also, the concentration gradient caused by the cation and anion transports in the electrolytes during cell operation results in the premature failures [7, 8]. Hence, the single ion conduction is the straightforward solution to the above problems. The use of layered silicate clay (such as montmorillonite (MMT), hecrorite, laponoite, etc.)-based nanocomposite controls the ion mobility and ensures single ion conduction in polymer nanocomposite electrolytes (PNCEs). The clay-layered silicate nanocomposite improves mobility of cation while reducing the mobility of anion drastically due to the intercalation of cations into the layered silicate where the bulky anions are not able to enter. Such a class of materials is termed as PNCEs. This innovative idea was put forward by Aranda and Ruiz-Hitzky [7], and it was popularized by Vaia et.al. [9]. Recently, a number of studies on PNCEs have been reported in the literatures [7–11]. It is believed that the ionic transport takes place in the amorphous phase as compared to the crystalline phase [12–14]. The low conductivity of the SPE is also attributed to its semicrystalline nature. Hence, the suppression of the crystallinity and creation of a stable

amorphous phase are another way of improving the conductivity. The most important advances in increasing the ionic conductivity of SPEs were brought in to the effect by the incorporation of suitable amounts of plasticizers [12–15]. Generally, low molecular weight, high dielectric constant polar organic solvents such as ethylene carbonate, propylene carbonate, polyethylene glycol (PEG), etc. are used as plasticizer. The low viscosity of the plasticizer decrease the T_g, lower the melting temperature of SPE that increases the amorphous content, and high dielectric constant of plasticizer helps better ion dissociation. The decrease in T_g results in an increase in the local chain flexibility [16], which is coupled to the ion mobility. In short, a plasticizer improves the electrical conductivity of SPE by (a) increasing the amorphous content of polymer electrolytes, (b) dissociating ion aggregates present in polymer electrolytes, and (c) by lowering the glass transition temperature. Most of the reports are related to either the effect of filler or plasticizer on the properties of polymer–salt complex. To the best of our knowledge, only a very few reports are available in the literature which discuss the combined effect of filler and plasticizer on polymer electrolytes [17–21]. In this paper, we report a systematic investigation on the effect of plasticizer on the microstructural/structural and electrical properties of the PNCEs. Further, an attempt has been made to establish a correlation between the microstructure and physical properties in this system.

Experimental details

Material preparation

The plasticized polymer nanocomposite electrolyte (PPNCE) films were prepared by a standard tape-cast technique using commercially available polyethylene oxide (PEO; Aldrich, M_W ~6×10^5), NaClO$_4$ (Fluka), and dodecyl amine modified Na$^+$-montmorillonite (DMMT) and PEG (Aldrich, M_W=200). We have used MMT clay as inorganic filler, which possess intercalation properties to suppress dual ion conduction. The MMT filler is modified with dodecyl amine so that the hydrophilic nature of the silicate layer is changed into hydrophobic, and the interlayer spacing expands. This indeed creates appropriate environment for the intercalation of polymer chains between the clay layers [10]. The details of the procedure for dodecyl amine modification of montmorillonite have already been reported elsewhere [22]. Stoichiometric amounts of PEO and NaClO$_4$ (EO/Na=25) were dissolved in dehydrated acetonitrile, and the solution was stirred thoroughly for 12 h. A previously optimized ratio (5 wt.%) [23] of the filler (DMMT) was then added to the complex solution and further stirred for 12 h. Finally, the plasticizer (weight percent of PEG in relation to PEO) was added and stirred

for another 12 h. The resulting solution was then cast using a self-designed tape caster and dried slowly at room temperature followed by the vacuum drying. The resulting films were then heated at ~40 °C for 3–4 h in order to remove residual solvents, and freestanding PPNCE thin films were obtained. The entire operation was carried out in an inert atmosphere inside a glove box. Though the samples were prepared for compositions represented as (PEO)$_{25}$–NaClO$_4$+5 wt.% DMMT+x wt.% PEG, x=0, 5, 10, 20, 30, 40, and 50, a better result was expected up to x=20 [19, 20].

Material characterization

The structural and microstructural properties of the PPNCEs films were studied with X-ray diffraction (XRD; Rigaku Miniflex with CuK$_{\alpha 1}$, λ=1.5405 Å radiation) and scanning electron microscope (SEM JOEL-JSM, model 5800F), respectively. Differential scanning calorimetry (DSC; Shimadzu DSC-50) with a low temperature measuring head and liquid nitrogen coolant were used to study glass transition temperatures. About 10 mg of samples was crimped in alumina pans inside the glove box (under argon atmosphere) and transferred to DSC cell for measurement. The samples were slowly cooled to −100 °C and then heated to 150 °C at the rate of 10 °C/min. The Al$_2$O$_3$ powder was used as a reference material. Fourier transform infrared (FTIR) spectra of the nanocomposites were recorded with a FTIR spectrometer (Thermo Nicolet Corporation, NEXUS −870). The impedance data of the cell stainless steel (SS)/ PPNCE/SS were collected using a computer-controlled impedance analyzer (HIOKI LCR Hi TESTER Model 3532) in the frequency range of 100 Hz to 1 MHz with oscillating level of 100 mV at different temperatures (room temperature to 150 °C). The impedance spectrum was used to obtain the dc conductivity. Though we did not carry out any experiments related to its mechanical properties of the samples, the sample is mechanically stable and flexible after even 4 years from the date of preparation.

Results and discussion

Structure and microstructure

The XRD patterns of the PPNCE films with different concentrations of plasticizer are shown in Fig. 1a. In the case of films with and without plasticizer, XRD patterns showed the characteristic reflections at 2θ ~5° for DMMT and at 2θ ~19° and 23° for PEO. For clarity of presentation of XRD data and gather information about the intercalation of polymer–salt complex and plasticizer into the nanometric channel of MMT, we have amplified the XRD pattern in the
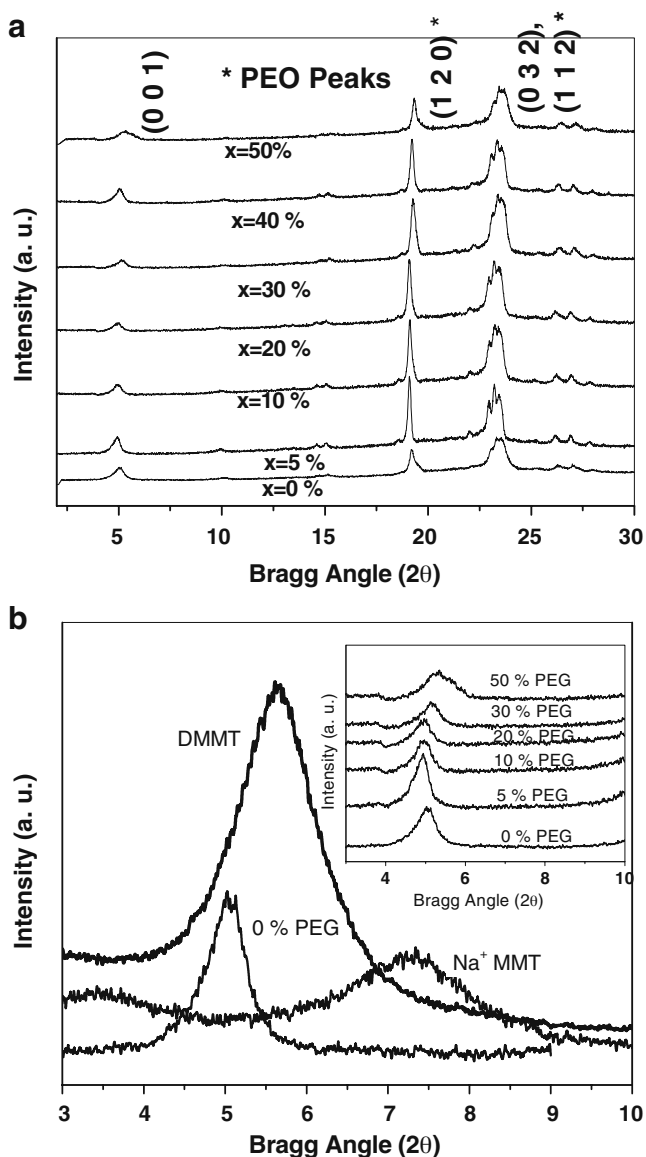
a XRD patterns of $(PEO)_{25}$–$NaClO_4$+5 wt.% DMMT+x wt.%

Fig. 1 **a** XRD patterns of $(PEO)_{25}$–$NaClO_4$+5 wt.% DMMT+x wt.% of PEG_{200}, with different value of x. **b** Amplified XRD patterns of Na^+ MMT, DMMT, and $(PEO)_{25}$–$NaClO_4$+5 wt.% DMMT+x wt.% of PEG_{200}, thin films in the range of 3–10° with different value of x

range of 3–10° with different value of x along with Na^+-MMT and DMMT (Fig. 1b). Intercalated clay layers of MMT exhibit relatively good crystalline organization along the c-axis as deduced from the (001) reflection in the XRD patterns [7, 8]. The distance between the clay sheets is given by d_{001} for (001) reflection. It is observed that Na^+-MMT (as received) exhibits reflection peak (001) at an angle $2\theta = 7.27°$ corresponding to the interlayer spacing (d_{001}) 12.15 Å, which include one clay layer of thickness 9.5 Å. The galley region therefore corresponds to 2.65 Å and contains Na^+-cation and water. Upon modification with dodecyl amine, the peak shifts toward the lower angle corresponding to interlayer spacing of 15.68 Å indicating the successful

intercalation of alkyl ammonium ion into the gallery of MMT. When DMMT is added to polymer–salt complex, there is an increase in the d_{001} (i.e., the peak position of (001) plane shift toward the lower angle side) indicating an increase in the gallery height of DMMT. The increase in the interlayer spacing corresponds to the increase in the gallery height, as the thickness of the layer is fixed. The MMT are capable of swelling and this gallery region can easily accommodate one or more layer of PEO. This clearly suggests the successful intercalation of polymer–salt complex into the gallery, which confirms the formation of nano-composites [7, 8]. Again on addition of plasticizer, the peak position of (001) shifts toward the lower angle up to 20% PEG concentration. On further increase in plasticizer concentration, it shifts toward the higher angle side. The structural parameters, calculated for the (001) reflection of DMMT and the main (120) reflection of PEO, are compared in Table 1. For different plasticizer concentrations, the corresponding interlayer spacing d_{001} ~17.50 Å as shown in Table 1. If the polymer is regularly intercalated, the value of d_{001} is close to 17.5 Å compared to 12 Å found for host silicate (hydrated sample containing a monolayer of H_2O). In the present study, the d value of (001) plane of the PPNCEs is ~17.5 Å, which indicates that the gallery height is ~8 Å. It is reported that the structure of PEO is a helix comprising of seven –CH_2–CH_2O– units [1]. When there is gallery height of ~8 Å, it is reported that the polymer helical conformation is retained inside the clay layers. So we can tell that the polymer chains are regularly intercalated between the silicate layers, which are consistent with the literature [7]. On addition of PEG, the peak position shifts toward the lower angle side is possibly due to the incorporation of the small plasticizer molecule in the interplanar spacing of the matrix of the polymer and DMMT [20]. Addition of plasticizer also brings substantial changes in the (120) reflection of PEO in the XRD patterns due to change in the crystallite size (L) of the PPNCE films (Table 1). From the table, it is observed that the interplanar spacing of the PEO with different plasticizer concentration is nearly same.

Table 1 Some structural parameters calculated from XRD data of $(PEO)_{25}$–$NaClO_4$+5 wt.% DMMT+x wt.% of PEG_{200}, with different PEG concentration

PEG concentration (x%)	MMT (001) peak		PEO peak (120)	
	d_{001} (Å)	L (nm)	d_{120} (Å)	L (nm)
0	17.50	14.15	4.64	28.3
10	17.87	15.7	4.64	39.0
20	17.91	14.8	4.64	39.9
30	17.27	14.5	4.59	30.2
40	17.58	16.8	4.61	40.8
50	–	–	4.58	35.0

Figure 2 shows scanning electron micrographs of PEO$_{25}$–NaClO$_4$+5 wt.% DMMT+x wt.% PEG for different values of x. A comparison of the surface morphology showed a marked change in the surface properties and the texture of the nanocomposite polymeric thin films on the addition of plasticizer. The micrograph of PPNCE ($x=0$%) showed (Fig. 2a) the presence of spherulites, which is characteristic of lamellar microstructure. The boundary between the spherulites is the amorphous phase regions. The spherulite showed the surface roughness that may be related to the crystalline fraction of the material. On addition of plasticizer, there was a decrease in the spherulite size and hence a substantial increase in the amorphous boundary region. Spherulites finally disappeared with higher plasticizer concentration ($\geq$20%). The surface roughness and the crystalline texture are decreased gradually on increasing concentration of plasticizer and ultimately resulted in very smooth texture of the surface. Therefore, plasticization helps in

reducing the crystallinity of the PPNCEs films, which is responsible for obtaining higher conductivity.

Glass transition temperature and fraction of free ions

DSC measurements were carried out to determine two important thermal parameters of semicrystalline polymer (i.e., glass transition temperature (T_g) and melting temperature (T_m)). Figure 3 shows the DSC patterns of the PPNCEs with different concentrations of plasticizer. The DSC curves displayed a step change corresponding to the glass transition temperature at low temperatures (Fig. 3a) and a predominant endothermic peak at high temperatures (Fig. 3b) corresponding to the melting of crystalline PEO region of the PPNCEs. Table 2 compiles the T_g and T_m values of PPNCEs for various plasticizer contents. It is clear from the table that T_g and T_m's got affected substantially on addition of the plasticizer. Both

Fig. 2 SEM micrographs of PPNCEs thin films of (PEO)$_{25}$–NaClO$_4$+5 wt.% DMMT+x wt.% PEG$_{200}$ with different concentration of x (i.e., **a** $x=0$, **b** $x=5$, **c** $x=10$, **d** $x=20$, **e** $x=30$, and **f** $x=50$)
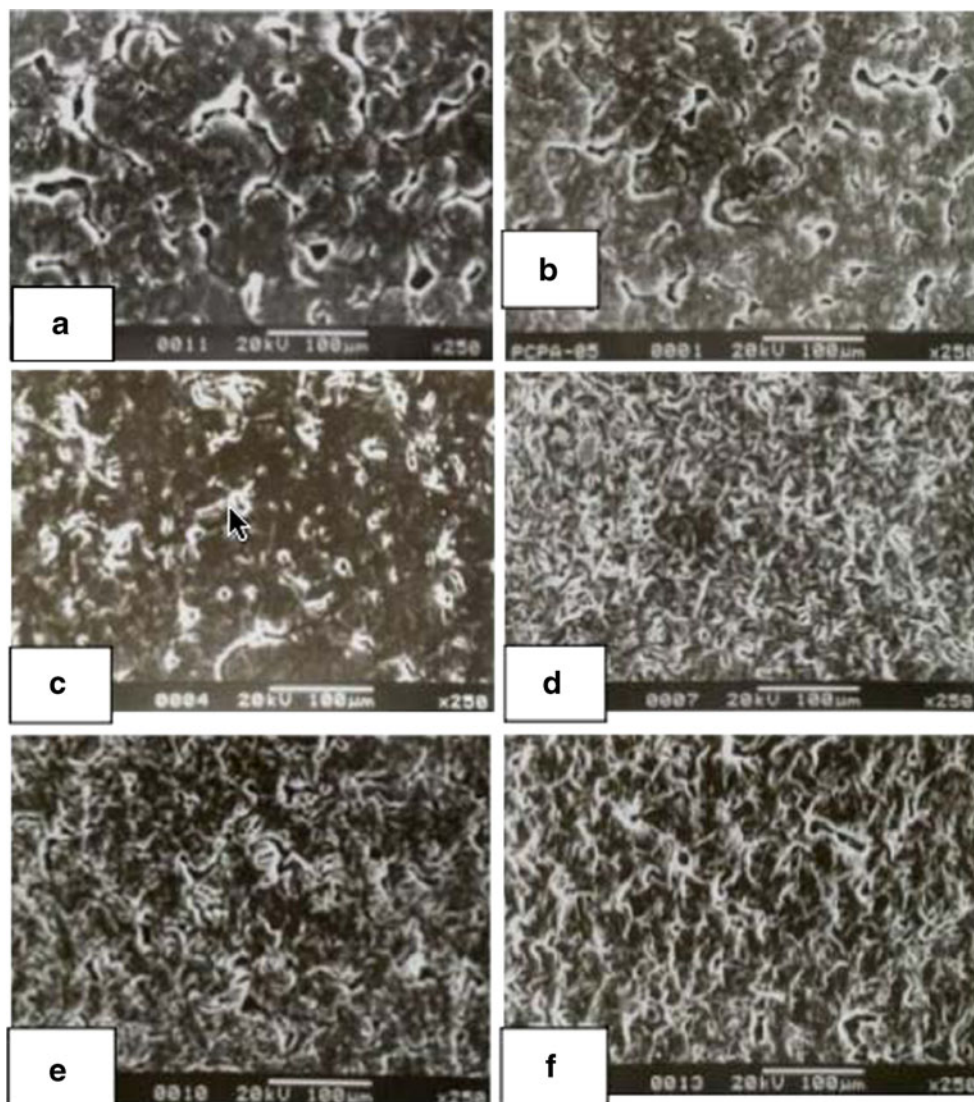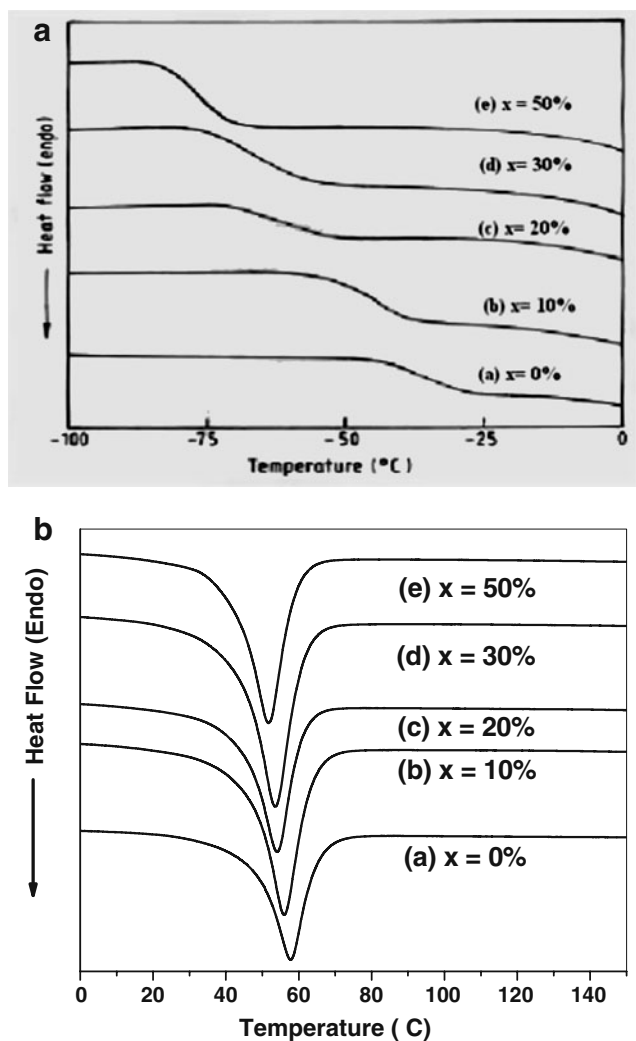
Fig. 3 DSC pattern in the temperature range of **a** −100 °C to 0 °C and **b** 0 °C to 150 °C of $(PEO)_{25}$–$NaClO_4$+5 wt.% DMMT+x wt.% of PEG_{200}, for different x (*a* $x=0$, *b* $x=10$, *c* $x=20$, *d* $x=30$, and *e* $x=50$)

T_g and T_m of PPNCEs shifted toward the lower temperatures on increasing plasticizer contents. It is well-known that T_g is a measure of the flexibility of the polymer chain; the lower is the T_g, the higher is the flexibility [13]. A decrease in the value of T_g helps easy movements of the polymer chains, which increases the conductivity as the

Table 2 Comparison of T_g (°C) and T_m (°C) of $(PEO)_{25}$–$NaClO_4$+ 5 wt.% DMMT+x wt.% nanocomposite electrolytes for different value of x

PEG concentration (x)	T_g (°C)	T_m (°C) peak
0	−35.84	57.84
10	−46.40	55.91
20	−61.64	54.23
30	−65.81	53.63
50	−76.07	52.00

ionic conductivity in polymer electrolytes is closely coupled to the polymer segmental mobility [1, 13, 16]. Therefore, it is expected that the addition of the plasticizer would have a positive influence on the ionic conductivity of the PPNCEs.

Figure 4 shows the FTIR spectrum of PPNCEs in the range 600–650 cm^{-1} related to the ν_4 mode of ClO_4^- ion for different plasticizer concentrations. The characteristic FTIR $\nu_4(ClO_4^-)$ mode of the sodium perchlorate $(NaClO_4)$ is particularly sensitive to the local environment in polymer electrolytes [24–26]. The fitting of ν_4 (ClO_4^-) envelopes yielded two contributions centered at ~623 and 635 cm^{-1}. Salomon and co-workers [25] have attributed the 623-cm^{-1} band to the spectroscopically free anions and 635-cm^{-1} band to the bound or contact ClO_4^- anions. According to them, the 623-cm^{-1} mode probably constitutes the solvent-separated ion pairs $Na^+(S)ClO_4^-$ (S stands for solvent) and solvent-separated dimmers. The 635-cm^{-1} band originates from contact or bound ion pairs. A commercially available peak fitting scientific software (PeakFit Version 4 Jandel) was used to separate $\nu_4(ClO_4^-)$ mode into two contributions. The sum of two Gaussian–Lorentzian product functions (i.e., pseudo-Voigt function) has been used to separate the contribution of "free" anions and contact ion pairs from raw FTIR data (Fig. 4). The fraction of "free" ion and contact ion pair has been calculated as the ratio of the integrated area under the peak attributed respectively to "free" anion and contact ion pairs to the total area for the $\nu_4(ClO_4^-)$ vibrations. Addition of PEG in the nanocomposite electrolytes had a profound influence on the fractions of free ions and the ion pairs.

Figure 5 shows the relative fractions of free ions with various concentrations of PEG. There is a monotonous increase in the relative fraction of the free ions on increasing PEG concentration. The plasticizers are generally low molecular weight and high dielectric constant materials. In this case, the low molecular weight plasticizer (i.e., PEG) posses high dielectric constant as compared to PEO, so that it is more polar as compared to the polymer host PEO. The high dielectric constant (i.e., polarizability) of plasticizer helps better ion dissociation. So the polar species are PEG in the present study. When plasticizer is added into PNCEs, the ion association becomes less favorable due to the increase in polarizability caused by the presence of such polar species. This results into a significant increase in the fraction of free ions on addition of PEG, as compared to that of polymer–salt complex and PNCEs.

Electrical properties

Electrical properties of PPNCEs with various amount of plasticizer were studied as a function of frequencies and

Fig. 4 Peak fitting of $\nu_4(ClO_4^-)$ FTIR internal modes for the PEO_{25}–$NaClO_4$+5 wt.% DMMT+x wt.% PEG system with different PEG concentration
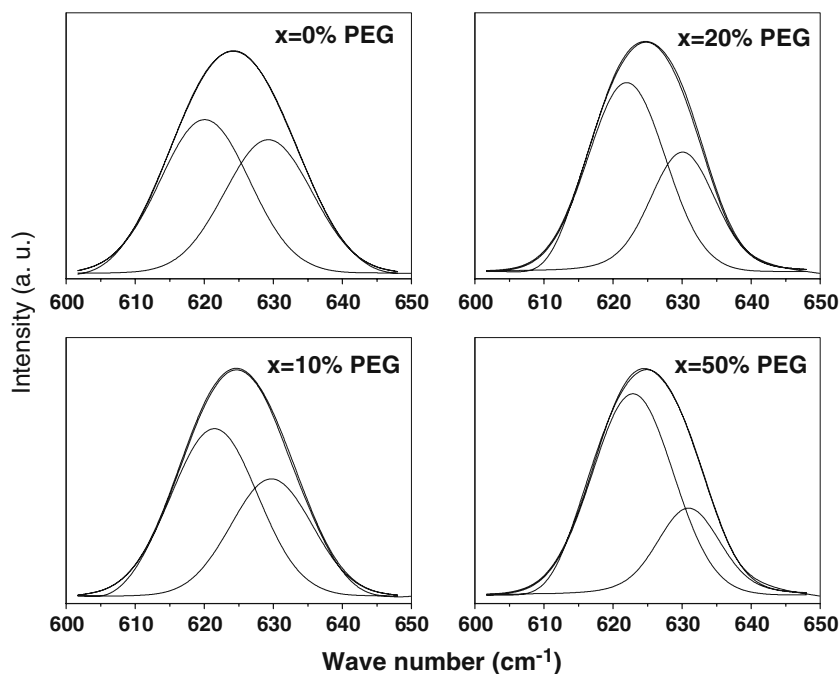
temperatures. The typical Nyquist plot of the all PPNCEs (Fig. 6) comprised of a broadened semicircle in the high-frequency region followed by a tail (spike) in the low-frequency region indicating a double-layer response (electrode/sample interface) [2, 27]. The higher frequency semicircle could be ascribed mainly to the bulk properties of the materials. The intercept of the semicircle with the real axis (Z') gives rise to the bulk (ionic) resistance (R_b) of the material. It is observed that the high-frequency semicircle fades away, and there is a reduction in the bulk resistance with increase in the plasticizer concentration. Hence, the plasticizer incorporation improves the ionic conductivity of PPNCEs.

The value of dc conductivity (σ_{dc}) of PPNCEs was calculated from the complex impedance spectra. Figure 7
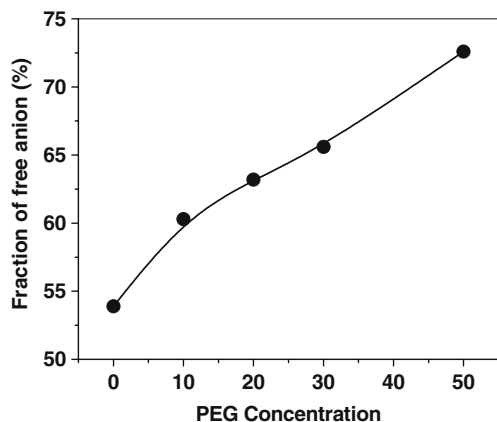
shows the variation of σ_{dc} at 40 °C as a function of plasticizer contents (x%) in the PPNCEs. The conductivity increases on increasing x and exhibits a plateau beyond $x\sim$ 20 wt.% of PEG. An enhancement in the value of conductivity by about one order of magnitude was found upon plasticizer addition as compared to that of the plasticizer free polymer nanocomposite electrolyte films. The maximum value of the conductivity obtained was $\sim4.4\times10^{-6}$ S cm^{-1} with $\sim$20% plasticizer contents in the polymer electrolyte. The variation of the conductivity as a function of plasticizer concentration can be rationalized in a
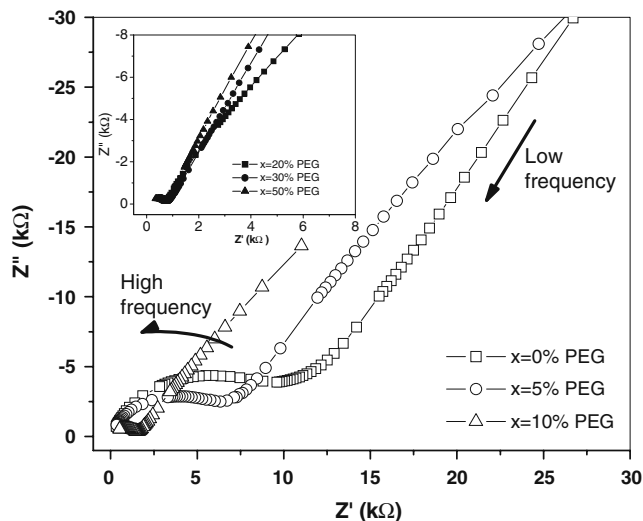

Fig. 5 Variation of fraction of free anion as a function of PEG concentration of PEO_{25}–$NaClO_4$+5 wt.% DMMT+x wt.% PEG

Fig. 6 Complex impedance spectrum of $(PEO)_{25}$–$NaClO_4$+5 wt.% DMMT+x wt.% PEG (x=0, 5, 10, 20, 30, and 50)
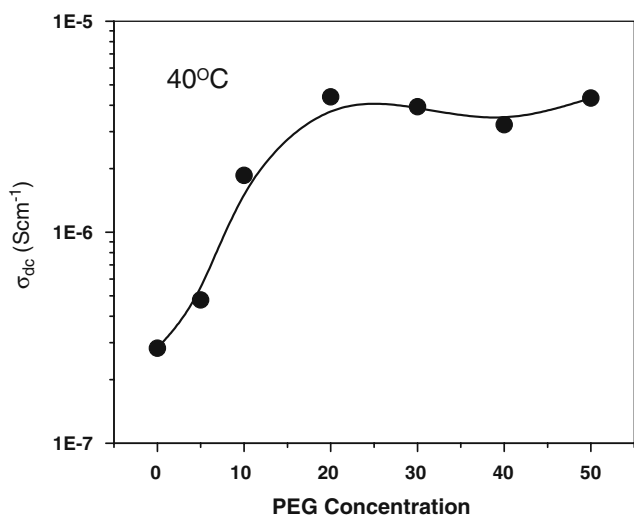
Fig. 7 Variation of dc conductivity (at 40 °C) as a function of plasticizer (PEG$_{200}$) concentration of (PEO)$_{25}$–NaClO$_4$+5 wt.% DMMT+x wt.% PEG

Fig. 8 Variation of dc conductivity as a function of temperature of (PEO)$_{25}$–NaClO$_4$+5 wt.% DMMT+x wt.% PEG with different concentration (x) of PEG

qualitative way as the conductivity; σ_{dc} of the polymer electrolyte is given by

$$\sigma_{dc} = \mu n q \qquad (1)$$

where n and μ are the charge carrier density and the mobility, respectively, and q is the charge. Mobility of the charge carrier is closely coupled to the segmental motion of the polymer chains, which is reflected by the glass transition temperature of the polymer electrolyte: The lower is the T_g, the higher is the segmental mobility [13]. The addition of plasticizer has a twofold influence on the conductivity: First, it leads to the increase in the free ion concentration (Fig. 5), which is responsible for the macroscopic conductivity, and secondly, it lowers T_g of the polymer electrolytes (Fig. 3a), thereby increasing the polymer chain mobility. In brief, each of the above two factors contribute positively toward the conductivity according to Eq. 1 and that predicts monotonous increase of the conductivity upon plasticizer addition, and it does not satisfactorily explain the conductivity variation at higher plasticizer concentration where the conductivity becomes almost independent of the plasticizer concentration. In the present system, 20% PEG was optimum plasticizer content for obtaining the highest conductivity (4.4×10^{-6} S cm^{-1}).

Figure 8 shows the variation of conductivity (σ_{dc}) as a function of temperature for various concentrations of plasticizers in PPNCEs. It is clearly seen from the figure that there were two distinct regions of conductivity, which are marked by the change of slope of the curve around 60 °C. Such type of temperature-dependent conductivity has been reported previously [17, 20, 23, 28]. The change in the slope of the conductivity curve above 60 °C resulted from the melting of the crystalline regions. Below the
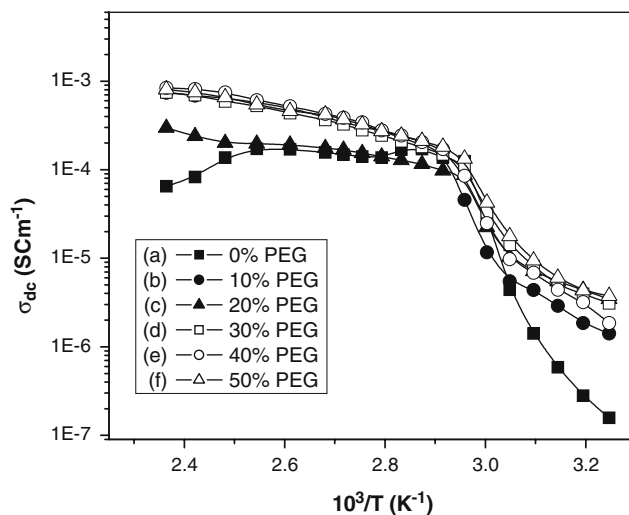
melting temperature, the conductivity did not strictly follow the Arrhenius behavior. This kind of temperature dependence of the conductivity is very common in polymer electrolytes and is best described by the typical Vogel–Tamman–Fulcher (VTF) relation [1, 2]:

$$\sigma = \sigma_0 \exp \frac{[-E_a]}{k_\beta[T - T_0]} \qquad (2)$$

where σ_0 is the pre-exponential factor, k_β=Boltzmann constant, E_a is the pseudoactivation energy, and T_0 is a reference temperature identified as the equilibrium glass transition temperature which is generally 50 K lower than that of the glass transition temperature.

Conclusions

Plasticized polymer nanocomposite electrolytes having heterogeneous combination (polymer–salt–filler–plasticizer) were synthesized. A significant effect of plasticization on structural, microstructure, thermal, and electrical properties of the PPNCEs has been observed in our study. The change in the surface morphology and increase in the amorphous content on addition of plasticizer has been investigated using SEM analysis. The introduction of plasticizer has the following effects on the PNCEs: (a) significant changes in the local structure/microstructure of the host medium, (b) enhances the fraction of amorphous phase, (c) improves the flexibility of the polymeric segments, and (d) releases of mobile charge carriers due to ion dissociation effect. The temperature dependence of the conductivity showed VTF pattern. An

enhancement in the conductivity by one order of magnitude has been observed upon plasticizer addition.

References

1. Gray FM (1997) Polymer electrolytes. RSC materials monographs. The Royal Society of Chemistry, Cambridge
2. MacCallum JR, Vincent CA (eds) (1987) Polymer electrolyte review—I & II. Elsevier, London
3. Rand DAJ, Woods R, Dell RM (1998) Batteries for electric vehicles. Wiley, New York
4. Conway BE (1999) Electrochemical supercapacitors: scientific fundamental and technological applications. Kluwer Academic, New York
5. Owen JR (1989) In: Lasker AL, Chandra S (eds) Superionic solids and solid electrolytes—recent trends. New York, Academic
6. Scrosati B (ed) (1993) Application of electroactive polymers. Chapman and Hall, London
7. Aranda P, Ruiz-Hitzky E (1992) Chem Mater 4:1395–1403
8. Pinnavaia TJ, Beall GW (eds) (2001) Polymer–clay nanocomposites. Wiley, New York
9. Vaia RA, Vasudevan S, Kkrawiec W, Scalson LG, Gannelis EP (1995) Adv Mater 7:154–156
10. Roy SS, Okamoto M (2003) Prog Polym Sci 28:1539–1641
11. Tjong SC (2006) Mat Sci Engg R 53:73–197
12. Berthier C, Gorecki W, Minier M, Armand MB, Chabgno JM, Rigaud P (1983) Solid State Ionics 11:91–95
13. Kumar M, Sekhon SS (2002) Eur Polym J 38:1297–1304
14. Tsutsumi H, Matsuo A, Onimura K, Oishi T (1998) Electrochem Solid-State Lett 1:244–245
15. Chen HW, Lin TP, Chang FC (2002) Polymer 43:5281–5288
16. MacFarlane DR, Sun J, Meakin P, Fasoulopoulos P, Hey J, Forsyth M (1995) Electrochim Acta 40:2131–2136
17. Pitwala HMJC, Dissanayake MAKL, Senevirante VA (2007) Solid State Ionics 178:885–888
18. Leo CJ, Subba Rao GV, Chowdari BVR (2002) Solid State Ionics 148:159–171
19. Pradhan DK, Samantaray BK, Choudhary RNP, Thakur AK (2005) Ionics 95(1 & 2):102
20. Pradhan DK, Samantaray BK, Choudhary RNP, Thakur AK (2005) J Power Sources 139:384–393
21. Wang YJ, Pan Y, Wang L, Pang MJ, Chen L (2005) Mater Lett 59:3021–3026
22. Bala P, Samantaray BK, Srivastava SK (2000) Mater Res Bull 35:1717–1724
23. Thakur AK, Pradhan DK, Samantaray BK, Choudhary RNP (2006) J Power Sources 159:272–276
24. Ducasse L, Dussauze M, Grondin J, Lassegues JC, Naudin C, Servant L (2003) Phys Chem Chem Phys 5:567–574
25. Salomon M, Xu M, Eyring EM, Petrucci S (1994) J Phys Chem 98:8234–8244
26. Woieczorek W, Lipka P, Zukowska G, Wycislik H (1998) J Phys Chem B 102:6968–6974
27. Macdonald JR (ed) (1987) Impedance spectroscopy, emphasizing solid materials and systems. Wiley Interscience, New York
28. Satiner M, Charles Hardy L, Whitmore DH, Shriver DF (1984) J Electrochem Soc 131:784–790